[CANCER RESEARCH 63, 8912–8921, December 15, 2003]

A Fully Human Monoclonal Antibody to the Insulin-Like Growth Factor I Receptor Blocks Ligand-Dependent Signaling and Inhibits Human Tumor Growth *in Vivo*

Douglas Burtrum, Zhenping Zhu, Dan Lu, Donna Marie Anderson, Marie Prewett, Daniel S. Pereira, Rajiv Bassi, Rashed Abdullah, Andrea T. Hooper, Henry Koo, Xenia Jimenez, Danielle Johnson, Robin Apblett, Paul Kussie, Peter Bohlen, Larry Witte, Daniel J. Hicklin, and Dale L. Ludwig

ImClone Systems Incorporated, New York, New York

ABSTRACT

The insulin-like growth factor I receptor (IGF-IR) is overexpressed in many diverse tumor types and is a critical signaling molecule for tumor cell proliferation and survival. Therapeutic strategies targeting the IGF-IR may therefore be effective broad-spectrum anticancer agents. Through screening of a Fab phage display library, we have generated a fully human antibody (A12) that binds to the IGF-IR with high affinity (4.11×10^{-11} M) and inhibits ligand binding with an IC_{50} of 0.6–1 nM. Antibody-mediated blockade of ligand binding to the IGF-IR inhibited downstream signaling of the two major insulin-like growth factor (IGF) pathways, mitogen-activated protein kinase and phosphatidylinositol 3′-kinase/Akt, in MCF7 human breast cancer cells. As a result, the mitogenic and proliferative potential of IGF-I and IGF-II were significantly reduced. A12 did not block insulin binding to the insulin receptor but could block binding to atypical IGF-IR in MCF7 cells. In addition, A12 was shown to induce IGF-IR internalization and degradation on specific binding to tumor cells, resulting in a significant reduction in cell surface receptor density. In xenograft tumor models *in vivo*, IGF-IR blockade by A12 was shown to occur rapidly, resulting in significant growth inhibition of breast, renal, and pancreatic tumors. Histological analysis of tumor sections demonstrated a marked increase in apoptotic tumor cells in antibody-treated animals. These results demonstrate that A12 possesses strong antitumor activity *in vitro* and *in vivo* and may therefore be an effective therapeutic candidate for the treatment of cancers that are dependent on IGF-IR signaling for growth and survival.

INTRODUCTION

Research and clinical studies have implicated the insulin-like growth factor I receptor (IGF-IR) and its ligands, insulin-like growth factor (IGF)-I and IGF-II, in the development, maintenance, and progression of cancer (1, 2). IGF-IR can stimulate cell proliferation, cell differentiation, changes in cell size, and protect cells from apoptosis. In tumor cells, overexpression of the receptor, often in concert with overexpression of IGF ligands, leads to potentiation of these signals and, as a result, enhanced cell proliferation and survival. IGF-I and IGF-II have been shown to be strong mitogens for a wide variety of cancer cell lines including prostate (3, 4), breast (5–8), colon (9–11), myeloma (12), melanoma (13), ovary (14), and lung (15), and this effect is mediated through the IGF-IR. High circulating levels of IGF-I in serum have been associated with an increased risk of breast, prostate, and colon cancer (16). Overexpression of IGF-II in cell lines and tumors occurs with high frequency and may result from loss of genomic imprinting of the *IGF-II* gene (17). In addition, highly metastatic cancer cells have been shown to possess higher expression of IGF-II and IGF-IR than tumor cells that are less prone to metastasize (18).

The principle pathways for transduction of the IGF signal are mitogen-activated protein kinase (MAPK) and phosphatidylinositol 3′-kinase/Akt (1, 19). After ligand-dependent receptor autophosphorylation, the IGF-IR phosphorylates a series of adaptor proteins, including insulin receptor substrate-1 (IRS-1), to activate intracellular signaling cascades. The MAPK pathway is primarily responsible for the mitogenic signal elicited after IGF stimulation but may also play a role in cell survival in cells overexpressing the IGF-IR (20). IGF-dependent signaling through phosphatidylinositol 3′-kinase elicits survival processes including the phosphorylation and activation of the antiapoptotic protein Akt and, as a result, has been shown to protect cells from damage-induced apoptosis (21). IGF signaling through the IGF-IR has also been shown to protect tumor cells from the cytotoxic effects of chemotherapy and radiation and may be an important factor in tumor cell drug resistance (5, 22). Furthermore, recent evidence suggests that resistance to the anti-HER2 antibody trastuzumab (Herceptin) in some forms of breast cancer may be due to activation of IGF-IR signaling in those cancers (23). Consequently, inhibition of IGF signaling has been shown to increase the susceptibility of tumor cells to chemotherapeutic agents, making it a logical target for therapeutic intervention (10, 24).

A variety of strategies have been developed to inhibit the IGF-IR signaling pathway in tumor cells. Approaches using antisense oligonucleotides, inhibitory peptide, soluble receptor, and dominant negative receptor mutants that target the IGF-IR have been effective at inhibiting the proliferation of tumor cell lines *in vitro* and in experimental mouse models (25–29). Murine antibodies directed against the human IGF-IR, in particular anti-IR-3, have also been shown to inhibit the proliferation *in vitro* and tumorigenesis *in vivo* of a variety of human tumor cell types (30–35). These studies have established targeting the IGF-IR as an attractive anticancer therapeutic strategy and validated an antibody approach as an effective mechanism to inhibit IGF-IR signaling. However, murine antibodies as such are not ideal human therapeutics, due to the high probability of developing specific immunity or allergic reactions to the therapeutic. Fully human antibodies offer the greatest potential for success as human therapeutics because they would be less likely to elicit an immune response and should possess a longer half-life *in vivo* (36). To this end, we have developed a fully human monoclonal antibody that specifically targets the human IGF-IR. We demonstrate that this antibody possesses high affinity for the receptor and acts as an antagonist of ligand binding and signaling. In addition, we show that this antibody is capable of facilitating the degradation of the IGF-IR after uptake and internalization, leading to a reduction in surface receptor density on treated tumor cells. As a result, this antibody exhibits strong antitumor cell activity *in vitro* and *in vivo*, demonstrating its potential as a candidate for antitumor therapy.

MATERIALS AND METHODS

Reagents and Cell Lines. Human recombinant extracellular IGF-IR and insulin receptor (IR) and ligands IGF-I, IGF-II, and insulin were purchased from R&D Systems Inc. (Minneapolis, MN). ^{125}I-IGF-I and ^{125}I-insulin were purchased from Amersham Biosciences (Piscataway, NJ). Reagent chemicals

Received 6/10/03; revised 10/1/03; accepted 10/9/03.

The costs of publication of this article were defrayed in part by the payment of page charges. This article must therefore be hereby marked *advertisement* in accordance with 18 U.S.C. Section 1734 solely to indicate this fact.

Requests for reprints: Dale L. Ludwig, Department of Molecular Biology, ImClone Systems Incorporated, 180 Varick Street, New York, New York 10014. Phone: (646) 638-5187; Fax: (212) 645-2054; E-mail: Dale.Ludwig@imclone.com.

were purchased from Sigma (St. Louis, MO). DNA modifying or restriction enzymes were from Fermentas (Hanover, MD). Cell culture media and reagents were obtained from Invitrogen/Life Technologies, Inc. (Rockville, MD), except FCS was obtained from HyClone (Logan, UT). Cell lines used in this study were obtained from American Type Culture Collection (Manassas, VA). MCF7 and T47D were cultured in DMEM containing 10% FCS and 2 mM glutamine. ZR-75-1, BxPC-3, RPMI-8226, and Colo205 were cultured in RPMI 1640 supplemented with FCS and glutamine. All cell lines were cultured in humidified incubators at 37°C in 5% CO_2.

Phage Display Screening. Recombinant extracellular human IGF-IR was used to screen a human naïve (nonimmunized) bacteriophage Fab library containing 3.7×10^{10} unique clones (37, 38). Soluble IGF-IR (50 μg/ml) was coated onto tubes and blocked with 3% milk/PBS. Phage were prepared by growing library stock to log phase, rescuing with M13K07 helper phage, and amplifying overnight at 30°C in 2YT culture medium containing ampicillin and kanamycin selection. The resulting phage preparation was precipitated in 4% polyethylene glycol/0.5 M NaCl and resuspended in 3% milk/PBS. Immobilized IGF-IR was incubated with the phage preparation for 1 h at room temperature, and tubes were washed 10 times with PBST (PBS containing 0.1% Tween 20) and with PBS. The bound phage was eluted with 1 ml of 100 mM triethylamine and allowed to infect log phase TG1 *Escherichia coli*. Infected TG1 cells were pelleted, spread onto selection plates, and incubated overnight at 30°C. Resulting colonies were pooled and stored in 2YT (10% glycerol) at –70°C. For second-round selection, this phage stock was used for enrichment of IGF-IR selective Fab following the above procedure, but with a reduced concentration of immobilized IGF-IR (5 μg/ml) and increased numbers of washes. Individual Fab candidates were rescued from selected TG1 clones as described above. Amplified phage preparations were blocked with 3% milk/PBS at room temperature for 1 h and added to Maxi-sorb 96-well microtiter plates (Nunc) coated with IGF-IR (1 μg/ml $\times$ 100 μl). After incubation at room temperature for 1 h, the plates were washed three times with PBST and incubated with a mouse anti-M13 phage horseradish peroxidase-conjugated antibody (Amersham Pharmacia Biotech, Piscataway, NJ). The plates were washed five times, tetramethylbenzidine (TMB) peroxidase substrate (KPL, Gaithersburg, MD) was added, and the absorbance at 450 nm was read using a microplate reader (Molecular Devices, Sunnyvale, CA). The diversity of anti-IGF-IR Fab clones was assessed by restriction analysis. Fab purification was performed as described previously (38).

Generation of Light Chain-Shuffled Phage Display Library. The human phage display library, from which anti-IGF-IR Fab 2F8 was identified, was used as the source of the antibody light chain repertoire in the shuffled library. A phagemid preparation from the Fab library was first digested with *Sfi*I and *Not*I, followed by electrophoresis on an agarose gel to delete the VH gene fragments from the antibody light chain-containing backbone vector. The gene encoding the VH domain of clone 2F8 was generated by digestion of 2F8-coding phagemid with the same restriction enzymes and gel purified. The 2F8 VH-coding gene was then ligated into the purified backbone vector to create the antibody light chain-shuffled Fab repertoire. TG1 cells were transformed with the ligation mixtures via electroporation with a BTX600 (BTX, Holliston, MA). The transformed TG1 cells were grown in 2YT media at 37°C for 60 min and plated onto 2YT agar plates containing 100 μg/ml ampicillin and 2% glucose (2YTAG). Resulting colonies were scraped into 5 ml of 2YTAG media, mixed with 50% glycerol to a final concentration of 10%, aliquoted, and stored at −70°C. Screening of the shuffled Fab library for IGF-IR binding was performed as described above, except that IGF-IR was coated at a concentration of 2 μg/ml.

BIAcore Analysis. The binding kinetics of soluble Fab and antibody proteins to IGF-IR was determined by using a BIACORE 3000 (BIAcore, Piscataway, NJ). Recombinant IGF-IR was immobilized onto a sensor chip, and Fab or antibody was injected at various concentrations. Sensorgrams were obtained and evaluated using BIA Evaluation 2.0 software to determine rate constants. The affinity constant, K_D, was calculated from the ratio of the rate constants K_{off}/K_{on}.

Solid Phase Receptor Binding Assays. Recombinant human IGF-IR or IR (100 ng/well) was coated onto 96 strip-well plates and blocked with 5% milk/PBS. Antibody preparations were diluted onto IGF-IR plates and incubated for 0.5–1 h at room temperature. Bound antibody was detected with a goat antihuman Fc-horseradish peroxidase antibody (Sigma) and visualized with TMB reagents and microplate reader at $A_{450\ nm}$. For competitive blocking assay, 40 pM ^{125}I-IGF-I or ^{125}I-insulin was added after antibody pretreatment, and the plates were incubated for an additional 90 min. Wells were then washed three times with ice-cold PBS/0.1% BSA, dried, and counted in a gamma scintillation counter. Anti-insulin blocking antibody 47-9 was obtained from NeoMarkers/LabVision (Fremont, CA).

Cell-Based Blocking Assay. Assays were performed as described previously (31), with minor modifications. MCF7 or ZR-75-1 human breast cancer cells were seeded into 24-well dishes and cultured overnight. Subconfluent monolayers were washed two to three times in binding buffer (Iscove's Medium/0.1% BSA), and antibody was added in binding buffer. After a short incubation with antibody or cold ligand on ice, 40 pM ^{125}I-IGF-I or ^{125}I-insulin (approximately 40,000 cpm) was added to each well and incubated for an additional 3 h with gentle agitation. The wells were then washed three times with ice-cold PBS/0.1%BSA. Monolayers were then lysed with 200 μl of 0.5N NaOH and counted in a gamma counter.

Antibody Engineering and Expression. The DNA sequences encoding the heavy and light chain genes from Fab candidates were amplified by PCR for cloning into glutamine synthetase system expression vectors (Lonza Biologics plc, Slough, Berkshire, United Kingdom). Engineered immunoglobulin expression vectors were stably transfected in NS0 cells using glutamine synthetase selection, and clones were screened for antibody expression by anti-Fc ELISA. Full-length IgG1 antibody was purified by protein A affinity chromatography (Poros A; PerSeptive Biosystems Inc., Foster City, CA).

Cell Proliferation and Mitogenesis Assays. For proliferation inhibition, 10,000 MCF7 cells were seeded into 24-well plates in complete medium. After 24 h, 50 nM antibody was added to plates in triplicate and allowed to culture for an additional 3 days. The mouse monoclonal antibody anti-IR-3 was obtained from Oncogene Science (Cambridge, MA). The total number of cells (bound and suspension) for each well was determined using a Coulter counter. Mitogenic assay was performed as described previously (39), with some modification. Human tumor cells were plated into 96-well tissue culture plates at 5,000–10,000 cells/well and allowed to adhere. RPMI-8226 cells were cultured in round-bottomed dishes and sedimented by gentle centrifugation before medium changes. The medium was replaced with serum-free medium and incubated overnight at 37°C. Cells were incubated with IGF-I with or without antibody and incubated overnight at 37°C. [^{3}H]Thymidine (0.25 μCi; ICN, Irvine, CA) was subsequently added to each well and incubated for 5 h at 37°C. The supernatant was aspirated, and the cells were suspended by trypsinization for 5 min. The cells were collected onto a filter and washed three times with water, using a cell harvester. After drying, the filter was processed for reading in a scintillation counter.

Western Blotting and Immunoprecipitation. Cells were plated into 10-cm or 6-well culture dishes and grown to 70–80% confluence. Monolayers were washed twice in PBS and cultured overnight in serum-free medium. Antibody was then added in fresh serum-free media and incubated at 37°C for 30–60 min. Cells were incubated with ligand for 10 min and then placed on ice and washed with ice-cold PBS. The cells were lysed in 50 mM Tris-HCl (pH 7.4), 150 mM NaCl, 1% Triton X-100, 1 mM EDTA, 1 mM phenylmethylsulfonyl fluoride, 0.5 mM Na_3VO_4, 1 μg/ml leupeptin, 1 μg/ml pepstatin, and 1 μg/ml aprotinin on ice for 10 min. The lysate was clarified by centrifugation at 4°C. Solubilized IGF-IR was then immunoprecipitated from the lysate. Antibody IGF-IRβ, clone C-20 (Santa Cruz Biotechnology, Santa Cruz, CA) or A12 at 4 μg/ml were incubated with 400 μl of lysate overnight at 4°C. Immune complexes were precipitated by the addition of protein A-agarose beads for 2 h at 4°C, pelleted, and washed three times with lysis buffer. For immunoprecipitation of pure IRs, IGF-IR-depleted supernatant from an IGF-IR immunoprecipitate was immunoprecipitated with anti-insulin antibody 18-44 (NeoMarkers/LabVision). Immunoprecipitates bound to the protein A-agarose beads were stripped into denaturing gel sample buffer. Lysates or immunoprecipitates were processed for denaturing gel electrophoresis and run on a 4–12% acrylamide gel and blotted to nitrocellulose membrane by Western blot. Tyrosine-phosphorylated protein was detected on the blot using an anti-phospho-tyrosine antibody (NeoMarkers/LabVision) and an antimouse-horseradish peroxidase secondary antibody. IGF-IR-β was detected with monoclonal antibody C-20 (Santa Cruz Biotechnology), and IR-β was detected using antibody CT-3 (Cell Signaling Technology, Beverly, MA). Phospho-Akt and total Akt antibodies were obtained from PharMingen (BD Biosciences, San Diego, CA). For MAPK phosphorylation, phospho-p44/42 and total p44/42 antibodies were purchased from Cell Signaling Technology). Phospho-

IRS-1 and total IRS-1 were detected with 2381 and 2382, respectively, from Cell Signaling. Bands were visualized with the enhanced chemiluminescence reagent (Amersham Pharmacia Biotech) on X-ray film (Eastman Kodak, Rochester, NY).

Antibody Internalization Assay. Antibody A12 was radioiodinated with ^{125}I [Amersham Pharmacia Biotech using IODO beads (Pierce, Rockford, IL)] according to manufacturer's instructions. MCF7 human breast cancer cells were plated into 6-well plates and cultured overnight to 70% confluence. One μg of ^{125}I-A12 was added to each well and incubated at 37°C or kept on ice at 4°C. Plates were incubated for 30, 90, or 180 min, and each time point was performed in triplicate. The control was held at 4°C for 180 min. At each time point, wells were washed three times with PBS/0.2% BSA and then stripped for 5 min with 100 mM glycine-HCl, 2 M urea (pH 2.5). Cells were washed three times with PBS/0.2% BSA and solubilized with 1N NaOH/1% Triton X-100. Stripped and solubilized fractions were then read on a gamma counter.

Receptor Degradation Analysis. MCF7 cells were plated in regular culture medium overnight followed by overnight incubation in serum-free medium. IGF-I (50 nM) or A12 was then added, and cells were incubated at 37°C for up to 24 h. Cells were washed in ice-cold PBS, lysed in radioimmunoprecipitation assay buffer, and quantitated by BCA kit (Pierce) for equivalent loading onto 4–12% Tris-glycine gels (Invitrogen). Proteins were electrophoresed and transferred to nitrocellulose membrane, and IGF-IR was detected using antibody C-20 against IGF-IRβ (Santa Cruz Biotechnology), antirabbit horseradish peroxidase-conjugated secondary antibody, and enhanced chemiluminescence reagent (Amersham Biosciences). Experiments including inhibitors were performed as described above, except that cells were pretreated with either 40 mM methylamine (Sigma) for 4 h or 30 μM MG115 (Sigma) or DMSO (Sigma) vehicle control for 2 h before the addition of ligand or A12.

Fluorescence-Activated Cell-Sorting Scanning of IGF-I Surface Receptor Density. Adherent MCF 7 cells were treated for 4 h with 50 nM of either IGF-I or A12 at 37°C. Cells were washed in ice-cold PBS/5% BSA twice, and 1×10^6 cells were aliquoted to staining tubes and placed on ice. Anti-IGF-IR antibody, Ab-1 (NeoMarkers, Fremont, CA), was then incubated with cells at 4°C for 2 h. After PBS/BSA washes, cells were incubated with antimouse IgG phycoerythrin-conjugated secondary antibody (PharMingen, BD Biosciences) for 1 h on ice. After PBS/BSA wash, cells were analyzed by fluorescence-activated cell-sorting assay using a FACSvantage SE flow cytometer (BD Bioscience).

Human Tumor Xenograft Models. Tumor xenografts were established by s.c. injection of 5×10^6 MCF7, 2×10^6 BxPC-3, or 2×10^6 Colo205 cells mixed in Matrigel (Collaborative Research Biochemicals, Bedford, MA) into the left flank of 5–6-week-old female athymic (nu/nu) mice (Charles River Laboratories, Wilmington, MA). In the MCF7 xenograft model, a pellet containing 0.72 mg of 17β-estradiol (Innovative Research of America) was implanted s.c. into the shoulder area of mice 3 days before tumor cell injection. Tumors were allowed to reach 150–300 mm^3 in size, and then mice were randomized into groups of 10 animals each. Mice were treated by i.p. injection every 3 days with vehicle control (saline) or monoclonal antibody A12 at a dose of 1 mg. Treatment of animals was continued for the duration of the study. Tumors were measured twice each week with calipers, and tumor volumes were calculated by the following formula: (π/6 (w1 $\times$ w2 $\times$ w2)), where w1 represents the largest tumor diameter, and w2 represents the smallest tumor diameter. Tumor volumes were analyzed using the Mann-Whitney *U* test and computed using the statistical package in SigmaStat (version 2.03; Jandel Scientific, San Rafeal, CA).

Immunohistochemistry of Tumor Sections. MCF7 tumor samples from representative animals were fixed in 10% neutral buffered formalin, embedded in paraffin, and sectioned at 4 μm onto slides. After deparaffinization and rehydration, sections were processed for H&E, Ki-67 or terminal deoxynucleotidyl transferase-mediated nick end labeling (TUNEL) staining. H&E-stained sections were stained with Gill's hematoxylin (VWR) and eosin (Richard Allen, Kalamazoo, MI). For Ki-67 staining, epitopes were unmasked at 95°C−99°C for 20 min in Target Retrieval Solution (DAKO, Carpinteria, CA). Endogenous peroxidases were blocked using Peroxidase Block (EnVision+ Rabbit System; DAKO) for 5 min at room temperature followed by a 1-h incubation at room temperature in nonspecific protein block (5% BSA, 10% normal goat serum, and 0.02% Tween 20). Ki67 was detected with antibody Ab-4 (LabVision, Fremont, CA) and 3,3′-diaminobenzidine+ per EnVision+ Rabbit System instructions. For detection of TUNEL-positive cells, the In Situ Cell Death Detection Kit (Roche Applied Science, Indianapolis, IN) was used per kit instructions with minor modifications. Briefly, sections were digested for 15 min at room temperature with proteinase K (20 μg/ml) and permeabilized with 0.1% sodium citrate buffer containing 0.1% Triton X-100 for 2 min at 4°C, followed by incubation with TUNEL labeling mix at 37°C for 1 h. After multiple washes, sections were counterstained with Hoechst 33342 (Molecular Probes, Eugene, OR) and coverslipped using an anti-fade reagent. Light and fluorescent images of immunostained tissue were viewed on a Zeiss Axioskop and digitized using a SONY camera and Scion CG-7 framegrabber. Proliferation index was determined by quantitation of Ki-67 immunostaining by calculating the number of 3,3′-diaminobenzidine-positive pixels/total number of nuclear pixels (hematoxylin-positive pixels plus 3,3′-diaminobenzidine-positive pixels) $\times$ 100 in 10 fields at $\times$200. The apoptosis index, determined by TUNEL staining, is calculated from the number of TUNEL-positive pixels/total number of Hoechst-positive pixels $\times$ 100 in 10 fields at $\times$200. The apoptosis/proliferation ratio equals the apoptosis index/proliferation index $\times$ 1000. For single-dose immunohistochemistry analysis, athymic nude mice received injection with 2×10^6 tumor cells mixed in an equal volume of Matrigel. When tumors reached approximately 300−400 mm^3, they received i.p. injection with a single dose of A12 (1 mg) or saline. Tumor samples from four animals were removed at time intervals after treatment, fixed in 10% neutral buffered formalin, embedded in paraffin, and sectioned at 4 μm onto slides for immunohistological analyses. Sections were stained with primary antibodies [polyclonal anti-IGF-IRβ (1:100; Santa Cruz Biotechnology), polyclonal anti-phosphorylated IGF-IR (Tyr^{1131})/IR (Tyr^{1146}; 1:50; Cell Signaling Technology), or polyclonal anti-phosphorylated p44/42 MAPK (Thr^{202}/Tyr^{204}; 1:150; Cell Signaling Technology)] and visualized as described above.

RESULTS

Selection and Engineering of Human Anti-IGF-IR Blocking Monoclonal Antibodies. To develop a fully human antibody antagonist to the human IGF-IR, we used a human naïve Fab phage display library containing $>10^{10}$ independent clones. Fab candidates that bound to immobilized recombinant soluble extracellular human IGF-IR were cross-screened for blocking activity against radiolabeled IGF-I. After two rounds of selection, 80% of independent clones were positive for binding to IGF-IR. Candidates that exhibited >30% inhibition of radiolabeled ligand binding to recombinant receptor were selected, and *in vitro* blocking titers were determined. Four clones were identified. Of these, only Fab clone 2F8 was shown to inhibit ligand binding by >50%, with an IC_{50} of approximately 200 nM (data not shown), and was selected for conversion to full-length IgG1 format.

Light and heavy chain variable regions from 2F8 Fab were amplified by PCR and cloned in-frame to human immunoglobulin constant region sequences for expression as full-length IgG1 in mammalian cells. Binding kinetic analysis (BIAcore) was performed on 2F8 IgG, and 2F8 was shown to bind to the IGF-IR with an affinity of 0.6–1 nM ($K_D = 0.6–1 \times 10^{-9}$ M; $K_{on} = 2.8 \times 10^5$ M^{-1}s^{-1}; $K_{off} = 1.8 \times 10^{-4}$ s^{-1}). Because the binding affinity of native IGF-I for the IGF-IR has been determined to be as high as 0.1 nM (40, 41), we sought to improve on the binding affinity of 2F8 to make it more competitive with ligand. A second-generation Fab phage library was generated in which the 2F8 heavy chain was conserved, and the light chain was varied to a diversity of $>10^8$ unique species. This method, termed light chain shuffling, has been used successfully to improve the affinity of selected antibodies for a given target antigen (42, 43). This library was screened for binding to the human IGF-IR, and the panning process was performed for a total of three rounds. To select for higher affinity Fab candidates, the concentration of immobilized receptor was reduced, and the length of washes before elution were increased substantially. Seven clones were analyzed after isolation, and all seven contained the same DNA sequence and restriction digest

profile. The single Fab species was designated A12. After conversion to IgG1, binding kinetic analysis was performed on A12. BIAcore analysis determined that the binding affinity of A12 for IGF-IR was 40 pM (0.04×10^{-9} M; $K_{on} = 7.2 \times 10^{5}$ $M^{-1}s^{-1}$; $K_{off} = 3.0 \times 10^{-5}$ s^{-1}) or approximately a 10-fold increase over 2F8. As a result of the increased affinity for receptor, A12 possessed greater binding activity in receptor-based ELISA (Fig. 1*A*). In turn, A12 also exhibited increased blocking activity of radiolabeled IGF-I ligand for immobilized IGF-IR (Fig. 1*B*.). A12 possessed similar blocking activity to cold IGF-I, with an IC_{50} of approximately 1 nM (0.15 μg/ml), but had significantly greater ligand blocking activity than 2F8 or IGF-II (IC_{50} = 6 nM).

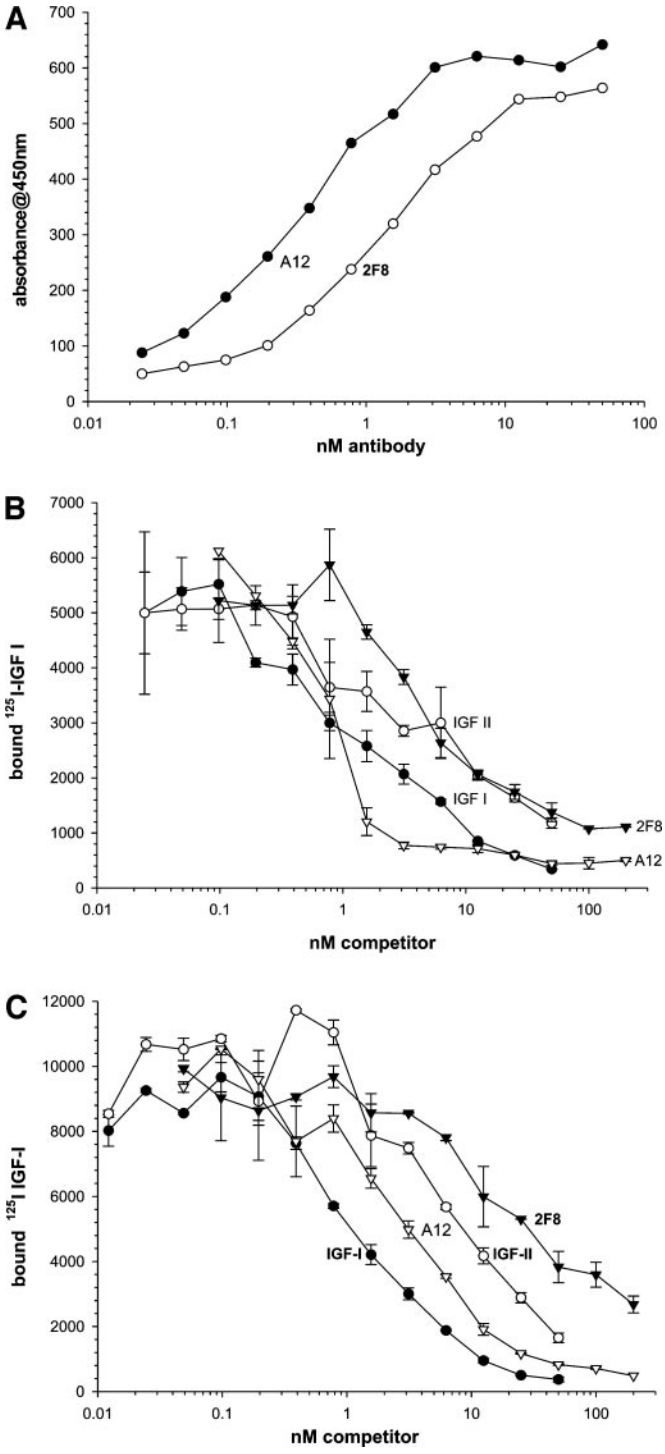

Fig. 1. Binding and blocking activity of anti-insulin-like growth factor I receptor (IGF-IR) antibodies. *A*, ELISA binding assay of 2F8 and A12 on immobilized recombinant human IGF-IR. ^{125}I-insulin-like growth factor (IGF)-I blocking activity of antibodies 2F8 and A12 or ligands IGF-I and IGF-II on (*B*) immobilized IGF-IR or (*C*) cultured MCF7 cells.

The antibodies were subsequently tested for competitive blocking of radiolabeled ligand to endogenous IGF-IR on human tumor cells. Using the human breast cancer cell line MCF7, which possesses a high IGF-IR density (44, 45), A12 inhibited ligand binding to cell surface IGF-IR with an IC_{50} of 3 nM (0.45 μg/ml; Fig. 1*C*). This was slightly lower than the inhibitory activity of cold IGF-I ligand (IC_{50} = 1 nM) but significantly better than the inhibitory activity of cold IGF-II (IC_{50} = 9 nM) and 2F8 (IC_{50} = 30 nM). The differences in observed activities for the two IGF ligands in these blocking assays can likely be attributed to the slower binding kinetics of IGF-II for the IGF-IR than ligand IGF-I (46).

A12 Inhibits Ligand-Dependent IGF-IR Phosphorylation and Downstream Signaling. Because it was demonstrated that anti-IGF-IR antibodies 2F8 and A12 possessed receptor antagonist activity on human tumor cells, as demonstrated by specific ligand blocking activity, we sought to determine the extent to which A12 inhibited receptor phosphorylation and activation of downstream effector molecules after ligand stimulation. Western blot analysis of receptor autophosphorylation and phosphorylation of Akt and MAPK (extracellular signal-regulated kinase 1/2) was performed in the presence or absence of antibody on the MCF7 human breast cancer cell line. As shown in Fig. 2*A*, autophosphorylation of the IGF-IR was arrested after serum deprivation, and the addition of either 2F8 or A12 alone did not induce receptor phosphorylation, indicating the absence of detectable antibody agonist activity at a concentration of 100 nM. On the addition of 10 nM IGF-I, IGF-IR phosphorylation was strongly induced. 2F8 effected an approximately 50% reduction in ligand-mediated IGF-IR phosphorylation, whereas A12 almost completely blocked phosphorylation.

Ligand-dependent signaling through the IGF-IR leads to tyrosine phosphorylation of the adaptor protein IRS-1, which in turn effects the downstream phosphorylation and activation of MAPK and phosphatidylinositol 3′-kinase/Akt. To determine whether A12 was equally capable of blocking signaling by IGF-I or IGF-II, we performed Western blots on cells treated with ligand in the presence or absence of A12 pretreatment. As shown in Fig. 2*B*, the levels of phosphorylated downstream effector molecules IRS-1, Akt, and MAPK in response to both IGF-I and IGF-II were significantly reduced in cells pretreated with A12. The extent of effector molecule inhibition was similar for both ligands, suggesting that A12 is equally proficient at blocking the signaling of both ligands to the IGF-IR.

A12 Does Not Block IR Signaling but Can Block Signaling of Atypical IGF-IR. The IGF-IR shares considerable homology with the IR (47). To demonstrate the selectivity of A12 for the IGF-IR, the antibody was tested in an IR blocking assay. As shown in Fig. 3*A*, A12 did not block the binding of radiolabeled insulin to the IR, even at 100 nM concentration. Cold insulin effectively competed with an IC_{50} of approximately 0.5 nM. A commercial anti-IR blocking antibody, 47-9, showed modest activity (50% maximal inhibition), and cold IGF-I competed only at high concentrations, consistent with previously published results (41). To further assess potential blocking of insulin binding on tumor cells, a blocking assay was performed on human breast cancer cell lines MCF7 and ZR-75-1. ZR-75-1 was included because it possesses a greater IR:IGF-IR ratio in comparison with MCF7 cells (44), and we reasoned that insulin binding to the cells would be more indicative of specific IR binding. MCF7 cells have been shown previously to possess atypical IGF-IR capable of high affinity binding of insulin (48). As shown in Fig. 3*B*, although cold insulin was able to titrate the binding of radiolabeled insulin to

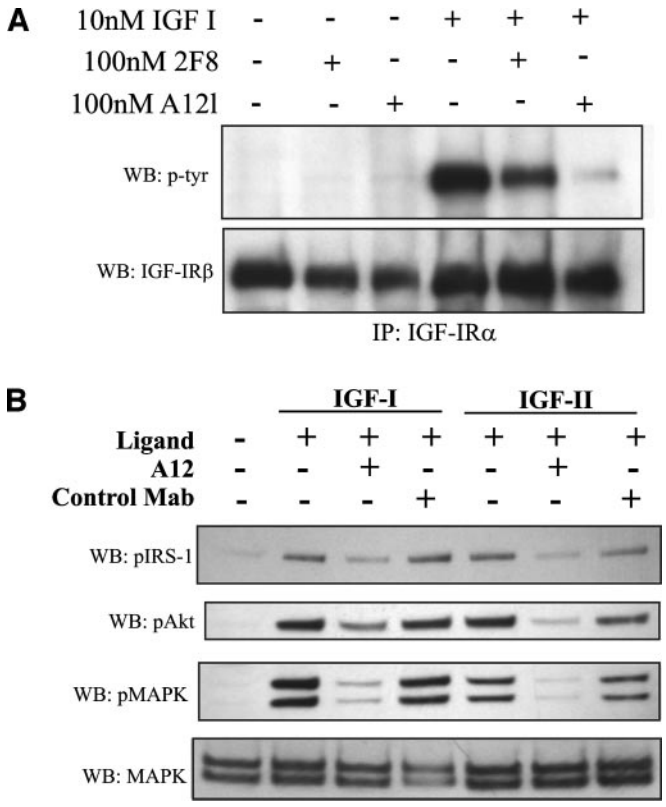

Fig. 2. Inhibition of ligand-dependent receptor autophosphorylation and signaling. *A*, MCF7 cells were pretreated with or without 2F8 or A12 (100 nM) before addition of insulin-like growth factor (IGF)-I (10 nM) for 10 min. Total receptor was immunoprecipitated (*IP*) with an anti-IGF-IR α chain-specific antibody and Western blotted (*WB*). Phosphorylated receptor was detected with an anti-phospho-tyrosine (*p-tyr*) antibody, and total receptor was detected with an insulin-like growth factor I receptor (IGF-IR) β chain-specific (*IGF-IRβ*) antibody. *B*, MCF7 cells were pretreated with or without 100 nM antibody (A12 or an irrelevant class-matched control) before addition of either IGF-I or IGF-II ligand (10 nM) for 10 min, and cell lysates were subsequently processed for Western blotting. Blots were probed for phosphorylated IRS-1 (*pIRS-1*), MAPK (*pMAPK*), and Akt (*pAkt*). For protein load control, lysates were blotted and probed for total MAPK.

cells, A12 did not block insulin binding to ZR-75-1 cells, even at an antibody concentration of 200 nM. As expected, A12 blocked insulin binding to MCF7 cells (Fig. 3*C*). To demonstrate selective blocking of IGF-IR and not IR by A12, we performed successive immunoprecipitation of IGF-IR and IR (44) in these cell lines to obtain only classical IR homodimers. Immunoblot analysis (Fig. 3*D*) showed no tyrosine phosphorylation of IRs in MCF7 cells by either IGF-I or insulin. To the contrary, tyrosine phosphorylation was induced by insulin but not IGF-I in ZR-75-1 and was not inhibited by A12. It could, however, be inhibited by the anti-IR blocking antibody 47-9. To assess further insulin signaling in MCF7 cells, we analyzed the IGF-IR/hybrid immunoprecipation for ligand-dependent signaling. As shown in the *bottom panel* of Fig. 3*D*, tyrosine phosphorylation of these receptors was induced by both IGF-I and insulin and inhibited by A12 but not 47-9. These results demonstrate that A12 selectively blocks IGF-IR receptors, including atypical and hybrid receptors, and does not block IRs on tumor cells.

A12 Mediates Rapid IGF-IR Surface Down-Modulation and Degradation. We sought to determine whether, on binding, A12 could mediate internalization and, consequently, degradation of the bound receptor. In MCF7 cells, radiolabeled A12 readily bound to the surface of tumor cells and was internalized in a time- and temperature-dependent fashion (Fig. 4*A*). To determine whether the antibody-bound internalized IGF-IR was degraded, resulting in surface receptor down-modulation, Western blots were performed on cells after prolonged treatment with A12. As shown in Fig. 4*B*, the level of IGF-IR was considerably reduced within 4 h after antibody treatment. To the contrary, receptor degradation was not apparent after treatment with IGF-I. To visualize potential changes in cell surface receptor density caused by antibody-mediated receptor degradation, we subjected MCF7 cells to fluorescence-activated cell-sorting analysis after incubation with A12 or IGF-I for 4 h at 37°C, staining for IGF-IR using an anti-polypeptide-specific nonblocking mouse monoclonal antibody. As shown in Fig. 4*C*, exposure to A12 effected a significant reduction in the fluorescence intensity of MCF7 cells, indicative of surface receptor down-modulation due to internalization. Calculated mean fluorescence intensity ratio indicated a reduction in IGF-IR surface staining of 90% after incubation with A12. This shift was not

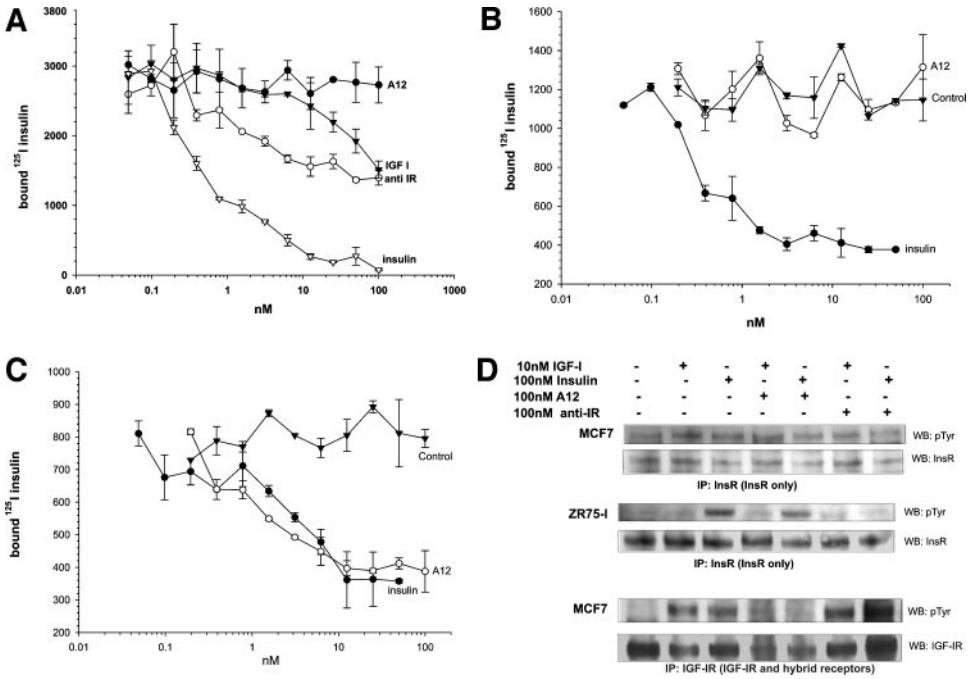

Fig. 3. Analysis of insulin blocking activity. *A*, ^{125}I-insulin blocking activity of cold insulin, cold insulin-like growth factor (IGF)-I, A12, or anti-IR antibody 47-9 (*anti-IR*) on immobilized recombinant IR. ^{125}I-insulin blocking activity of A12, control antibody, or cold insulin on (*B*) ZR-75-1 breast cancer cells or (*C*) MCF7 breast cancer cells is shown. *D*, immunoprecipitation and Western blot analysis of insulin-like growth factor I receptor (IGF-IR) and insulin receptor (IR) phosphorylation in breast cancer cells after stimulation with insulin or IGF-I in the presence or absence of blocking antibodies. To isolate classical IR from cells, cell lysate was first cleared of IGF-IRs and hybrids by immunoprecipitation with an IGF-IR-specific antibody and then immunoprecipitated with an IR-specific antibody. To visualize insulin-dependent signaling of atypical IGF-IR, the IGF-IR immunoprecipitate from MCF7 cells was also run. Phosphorylated receptor was detected with a phosphotyrosine-specific antibody, and total IR or IGF-IR was detected with IR or IGF-IR β subunit-specific antibody, respectively.

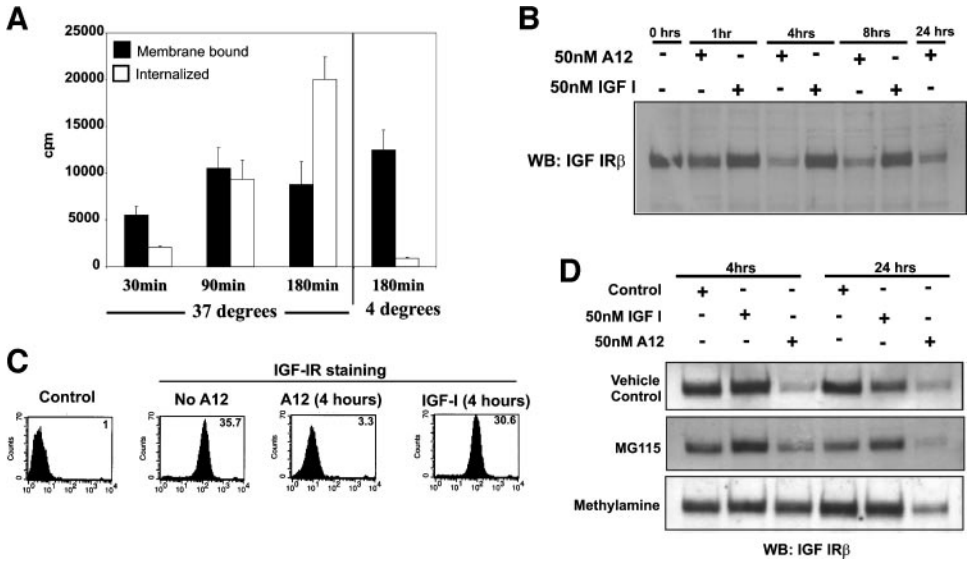

Fig. 4. Antibody induction of receptor internalization and degradation. *A*, A12 was radiolabeled with ^{125}I and incubated with MCF7 cells at either 37°C or 4°C. At the times specified, cells were washed with ice-cold PBS, and membrane-bound antibody was stripped, collected, and counted. Cells were lysed with NaOH and counted, representing internalized antibody. *B*, MCF7 cells were treated with either insulin-like growth factor (IGF)-I or A12 (50 nM) for the times indicated, and total cell lysate was prepared and quantitated. Equal lysate sample loads were separated by gel electrophoresis and processed for Western blotting. Total insulin-like growth factor I receptor (IGF-IR) was identified with an IGF-IR β chain-specific antibody. *C*, fluorescence-activated cell-sorting analysis of MCF7 cells stained for surface expression of IGF-IR. Cells were stained with anti-IGF-IR antibody and goat antimouse IgG phycoerythrin-conjugated secondary antibody after a 4-h incubation with 50 nM A12 or IGF-I at 37°C. Control cells were stained only with secondary antibody. *Numbers* indicate the mean fluorescence intensity ratio of the IGF-IR-positive peak relative to the control. *D*, MCF7 cells were pretreated with the proteosome inhibitor MG115, the lysosome inhibitor methylamine, or vehicle control before treatment with either IGF-I or A12 (50 nM) for 4 or 24 h. Total cell lysate was prepared and quantitated. Equal sample loads were then processed for Western blotting. Total IGF-IR was detected with an IGF-IR β chain-specific antibody.

seen when cells were incubated with A12 at 4°C, consistent with an energy-dependent, antibody-mediated, receptor internalization process (data not shown; refer to Fig. 4*A*). Exposure of cells to IGF-I did not cause a significant change in surface IGF-IR fluorescence intensity, consistent with Western blot analysis showing little effect of ligand on IGF-IR degradation (Fig. 4*B*).

To further assess the mechanism by which A12 could effect degradation of the IGF-IR, we treated cells with lysosome or proteosome inhibitors before exposure to A12. As shown in Fig. 4*D*, the lysosome inhibitor methylamine, but not the proteasome inhibitor MG115, substantially reduced the extent of antibody-mediated receptor degradation, indicating that receptor degradation occurs by a lysosome-dependent pathway. A significant level of degradation was, however, apparent in A12-treated samples at 24 h that were pretreated with methylamine, suggesting that other processes, in addition to lysosomal compartmentalization, are also likely involved in antibody-mediated receptor degradation.

A12 Inhibits IGF-Dependent Cell Mitogenesis and Proliferation. To determine whether A12 was capable of inhibiting ligand-dependent cell proliferation as a result of receptor blocking and down-modulation activity, a mitogenic assay was performed on MCF7 cells (Fig. 5*A*). Ligand was titrated on cells to determine the dynamic range of ligand stimulation and the relative amount of ligand necessary to achieve maximal mitogenic response (5–10 nM). Concentrations of A12 from 100 nm were tested and shown to inhibit breast cancer cell mitogenesis in response to IGF-I ligand in a dose-dependent fashion, with an IC_{50} value of 5 nM. MCF7 cells treated with A12 in the absence of ligand failed to stimulate mitogenesis (Fig. 5*B*), demonstrating that this antibody lacks detectable receptor agonist activity. We then tested the effect of A12 on inhibiting tumor cell growth in culture. Proliferating cells in culture in serum-containing medium were treated with 50 nM A12, mouse anti-IGF-IR monoclonal antibody anti-IR-3, or a control antibody and incubated for 4 days. Total cell number was then determined, and the calculated number of cell doublings was determined. Anti-IR-3 was included in this proliferation assay for comparison of IGF-IR antagonist activity. As seen in Fig. 5*C*, A12 effected a significant inhibition of MCF7 cell proliferation compared with control and anti-IR-3. In serum-containing medium, A12 inhibited proliferation of MCF7 cells by 90%, in comparison with 60% inhibition with anti-IR-3. To demonstrate broad inhibitory activity on multiple tumor types, we further tested A12 in mitogenic assays on several other diverse tumor types, including a second breast cancer line (T47D), a pancreatic cancer line (BxPC-3), and a multiple myeloma cell line (RPMI-8226). As shown in Fig. 5, *D–F*, A12 effected significant antimitogenic activity on each of these lines, with IC_{50}s of 10 nM or less. The fold induction of these cells in response to IGF-I ligand stimulation ranged from 1.3-fold (T47D) to 4-fold (BxPC-3).

Antitumor Activity of Antibody A12 in a Xenograft Tumor Model. A12 exhibited strong inhibitory activity on the IGF-dependent mitogenic stimulation and proliferation of tumor cells *in vitro*. To assess its activity on tumor growth *in vivo*, xenograft tumor models in athymic nude mice were used. Three IGF-IR-positive cell lines were selected for tumor study: MCF7 (breast cancer); BxPC-3 (pancreatic cancer); and Colo205 (colon cancer). Tumors were allowed to grow to at least 150 mm^3 before antibody treatment was initiated. Dose-response analysis was first performed in the MCF7 breast cancer model, using doses of 0.01, 0.1, and 1 mg, and tumor volumes were measured at regular intervals. As shown in Fig. 6*A*, A12 treatment of animals effected a dose-dependent inhibition of MCF7 tumor cell growth. Statistical significance between A12-treated and saline control tumor size was noted with 1 mg and 0.1 mg dosing, but not with 10-μg treatment. Because single-agent use of A12 effected complete inhibition of MCF7 tumor growth with 1 mg of antibody, dosing at 1 mg was used for subsequent studies with pancreatic and colorectal tumor lines. In the BxPC-3 pancreatic cancer model (Fig. 6*B*), A12 effected an 80% inhibition in tumor growth. As demonstrated in mitogenic assay, this line was quite responsive to IGF-I stimulation *in vitro*, and A12 treatment exhibited a major inhibitory effect on tumor growth *in vivo*. A12 also demonstrated significant antitumor activity

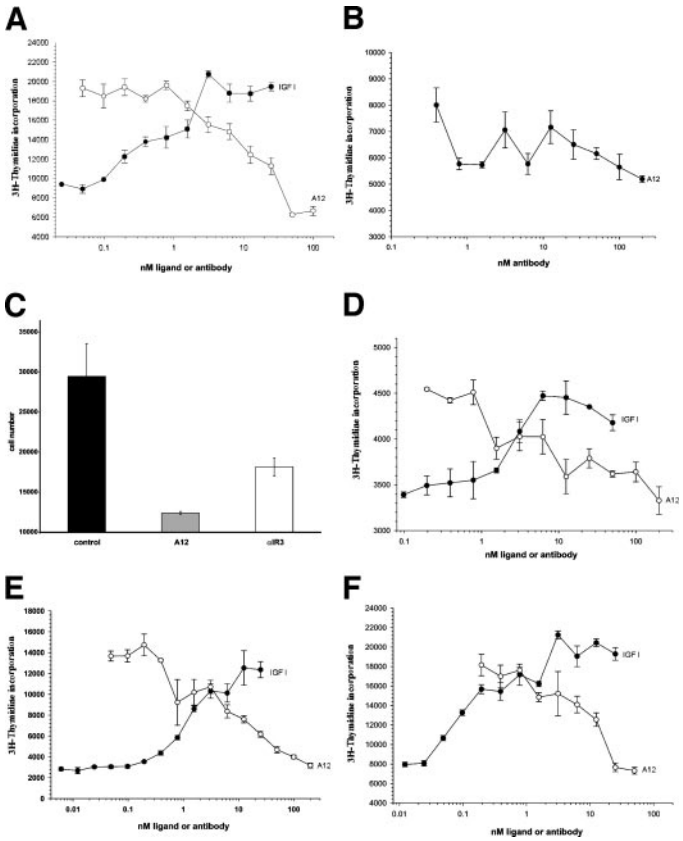

Fig. 5. Inhibition of tumor cell mitogenesis and cell proliferation by anti-insulin-like growth factor I receptor (IGF-IR) antibody. *A*, MCF7 cells were serum starved overnight and then incubated with or without insulin-like growth factor (IGF)-I or A12. For ligand mitogenesis, IGF-I was titered down from 25 nM and incubated overnight. For antibody titration, A12 was titered from 100 nM together with 10 nM IGF-I and incubated overnight. Cells were then treated with [^{3}H]thymidine for 5 h at 37°C and processed for [^{3}H]thymidine incorporation. *B*, MCF7 cells were treated with A12 titration as described in *A*, except that no IGF-I was added, to assess receptor agonist activity. Assay was performed concurrently with the experiment detailed in *A*. *C*, effect of antibody blockade of IGF-IR on MCF7 cell proliferation. Cells (10,000) were cultured in serum-containing medium with or without 50 nM antibody (A12 or anti-IR-3). After 3 days of incubation, total cell number was determined. The results depict the average of three independent platings, with SE shown, and are representative of multiple experiments. *D–F*, mitogenic assay performed as described in *A*, on human tumor lines T47D (breast cancer; *D*), BxPC-3 (pancreatic cancer; *E*), and RPMI-8226 (multiple myeloma; *F*), respectively.

in a xenograft model for colon cancer, Colo205 (Fig. 6*C*), effecting >70% inhibition of tumor growth. In none of the studies was any treatment-related toxicity or change in body weight noted in comparison with the saline-treated control animals. We have recently determined that A12 lacks any detectable antibody-dependent cellular cytotoxicity activity on three different IGF-IR-positive tumor lines including MCF7 (data not shown). The strong antitumor effect of A12 is therefore a direct result of its antagonism of IGF-IR signaling and is not due to effector function mechanisms.

To understand the processes by which tumor growth was inhibited by A12 targeting of the IGF-IR *in vivo*, histological analysis was performed on tumor sections from the MCF7 tumor model, and tumor sections were stained for markers of cell proliferation and apoptosis. As shown in Fig. 7*A*, numerous cancer cells with pyknotic nuclei were apparent in H&E-stained sections from tumors treated with 1 mg of A12 (Fig. 7*A*) in comparison with vehicle control-treated tumors, indicative of programmed cell death. Staining for the proliferation marker Ki67 demonstrated a noticeable decrease in the level of proliferating cells in the antibody-treated tumors. Consistent with the observation of higher levels of pyknotic nuclei in antibody-treated H&E-stained sections, TUNEL staining detected an increase in apoptotic cells in antibody-treated tumors (Fig. 7*A*). The levels of proliferating and apoptotic cells in these tumor sections were quantified by digital imaging analysis. As shown in Fig. 7*B*, there was a 20% reduction in the level of proliferative cells in antibody-treated tumors. To a greater extent, A12 caused a 6-fold increase in the number of apoptotic cells in antibody-treated tumors. The calculated ratio of apoptotic:proliferating cells in A12-treated samples was nearly 10-

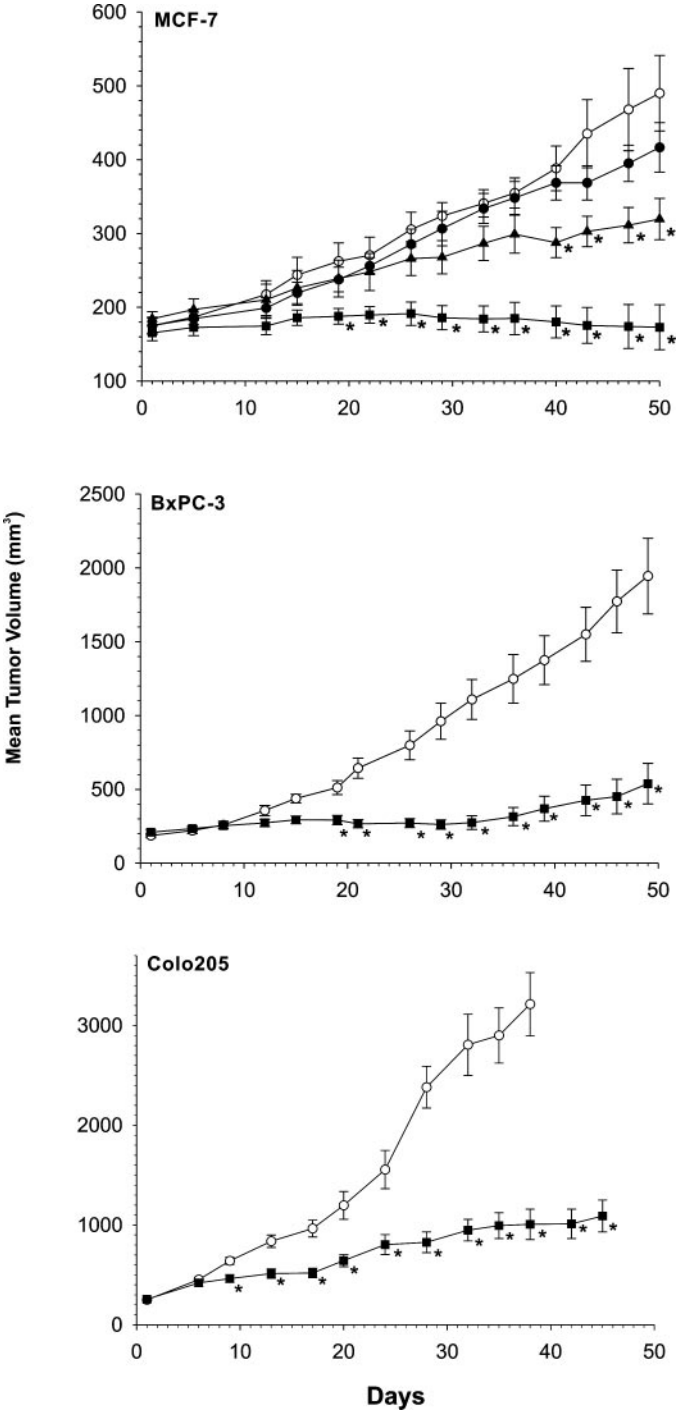

Fig. 6. Inhibition of tumor growth *in vivo*. MCF7, BxPC-3, or Colo205 tumor cells were injected s.c. as a Matrigel suspension into nude mice and allowed to grow to at least 150 mm^3. Groups of 10 animals each were treated with vehicle control (saline; ○) or A12 in saline every 3 days. For MCF7, a dose-escalation study was performed using antibody treatments of 10 μg (●), 100 μg (▲), or 1 mg (■). BxPC-3 and Colo205 received 1-mg doses of A12 (■). Tumor size was measured with calipers at regular intervals. SE is shown for each point on the graph. Statistics were performed by Student's *t* test, and significance ($P < 0.05$) relative to control is noted in the graph (*).

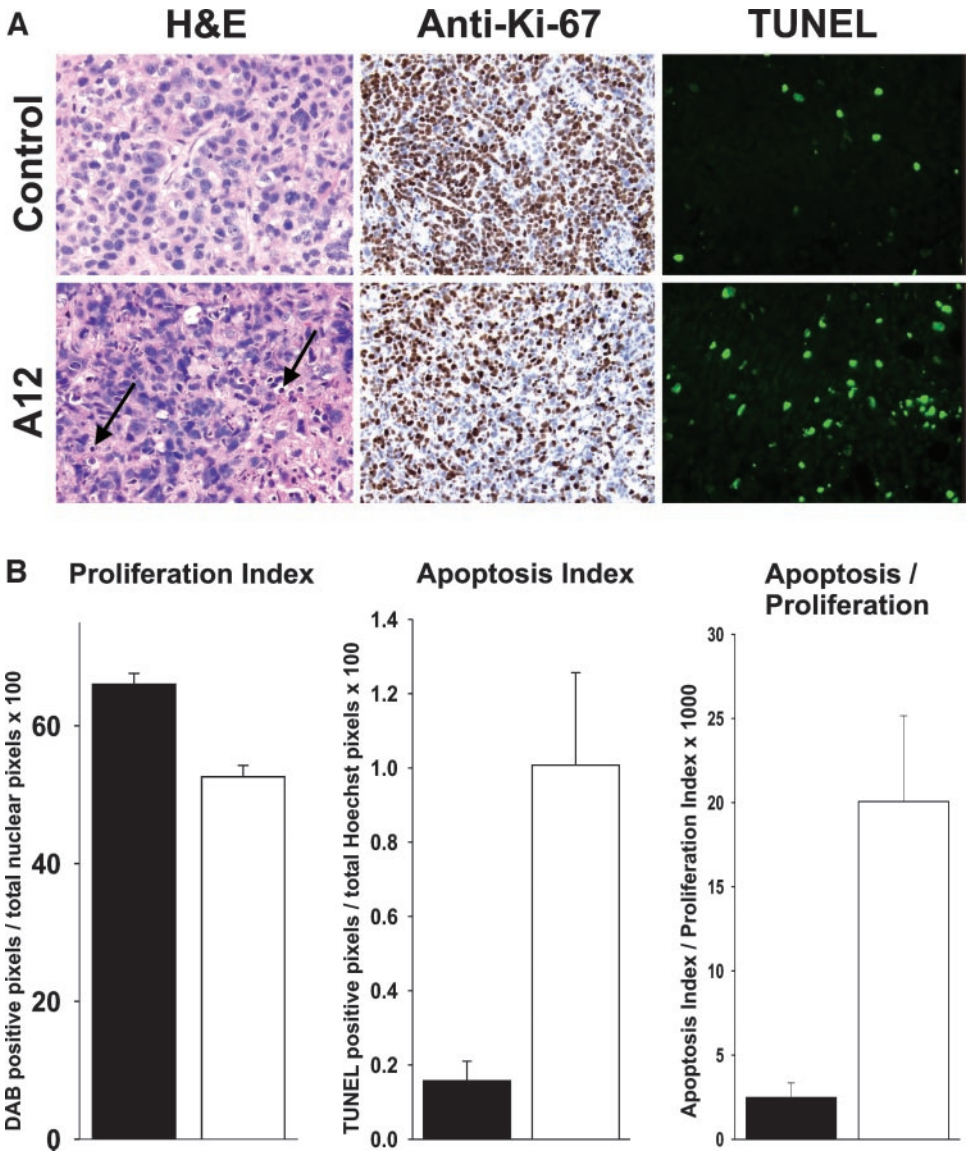

Fig. 7. Histological analysis of tumor sections from A12-treated MCF7 xenograft tumor model. Tumor samples from representative animals were resected, fixed, and processed for H&E, anti-Ki67 immunohistochemistry, and terminal deoxynucleotidyl transferase-mediated nick end labeling (TUNEL) analyses. *A*, antibody-treated samples were shown to possess noticeable levels of pyknotic nuclei above vehicle controls (*arrows*; ×400). A modest yet significant inhibition of Ki67 staining was apparent in the antibody-treated sections (×200). Extensive TUNEL-positive cells were apparent in the antibody-treated sections, whereas little staining was observed in the control sections (×400). *B*, quantitation of the proliferation index revealed a significant 20% reduction in staining over control groups. Proliferation index is expressed as the number of 3,3′-diaminobenzidine (*DAB*)-positive pixels divided by the total number of nuclear pixels (hematoxylin-positive pixels plus 3,3′-diaminobenzidine-positive pixels) in 10 fields at ×200/animal, 2 animals/group. Quantitation of the apoptosis index demonstrated a significant 6-fold increase in TUNEL reactivity after antibody treatment as compared with controls. Apoptosis index is expressed as the number of TUNEL-positive pixels divided by the total number of Hoechst-positive pixels, multiplied by 100, in 10 fields at ×200/animal, 2 animals/group.

fold greater than that in control tumors, suggesting that as a result of A12 treatment, a combined induction of programmed cell death and a reduction in the proliferation rate of tumor cells were responsible for the dramatic inhibition of tumor growth *in vivo*.

We subsequently sought to assess the processes of receptor down-modulation and signaling inhibition in tumors *in vivo* to demonstrate that the mechanism of action by which A12 exerts it antitumor effect is consistent with the *in vitro* antiproliferative results we observed in multiple human tumor cell lines. We performed immunohistochemical analysis on established BxPC-3 tumors at time intervals after a single 1-mg i.p. injection of A12. As shown in Fig. 8, total IGF-IR, phospho-IGF-IR, and phospho-MAPK were all markedly reduced within 6 h of A12 treatment. Within untreated samples, nearly all tumor cells stained positive for these markers. The speed with which receptor down-modulation occurred in tumors was consistent with that observed *in vitro* (Fig. 4), and a noticeable reduction in total IGF-IR and pMAPK was apparent within 1 h after A12 treatment. Despite repeated attempts, BxPC-3 tumor sections failed to stain for pAkt and thus could not be evaluated in this study. These results, however, demonstrate that A12 is a potent antagonist of IGF-IR signaling, inhibiting both receptor and effector molecule phosphorylation *in vivo* through a combination of ligand blocking and receptor down-modulation. As a result, A12 was shown to significantly inhibit tumor growth and proliferation.

DISCUSSION

This paper describes the successful generation of a high-affinity fully human monoclonal antibody, A12, that binds specifically to the human IGF-IR and blocks IGF-I and IGF-II signaling. Importantly, A12 and its precursor, 2F8, did not block binding of insulin to the IR. Both antibodies were shown to inhibit ligand-mediated receptor phosphorylation and downstream cellular signaling through the MAPK and Akt pathways. A12 was determined to be a potent inhibitor of IGF-I-mediated mitogenesis in the human breast cancer cell line MCF7 ($IC_{50} < 10$ nM) and was more effective than the mouse monoclonal antibody anti-IR-3 at inhibiting the proliferation of MCF7 cells in serum-containing medium. Furthermore, A12 did not exhibit receptor agonist activity in culture in either mitogenic or receptor phosphorylation assay. Certain inhibitory antibodies, including anti-IR-3, have been reported to act as weak agonists at high antibody concentrations (30, 49–51). A12 was shown to be an antagonist of both IGF-I and IGF-II binding and activation of IGF-IR. It has been shown that IGF-II is frequently overexpressed in human tumors, often

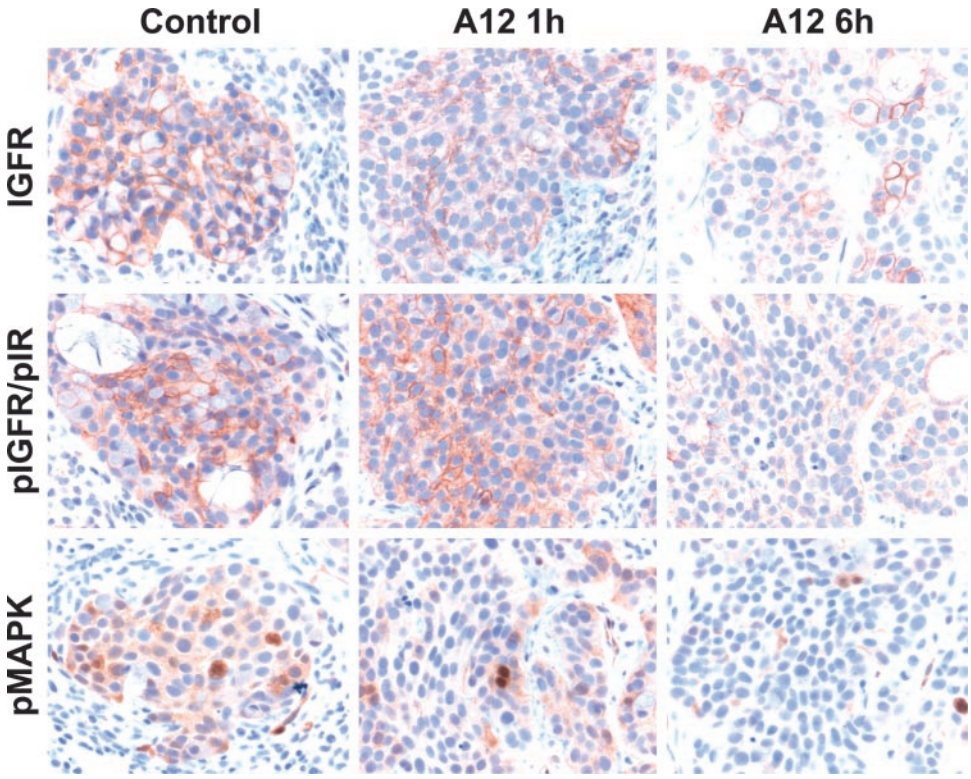

Fig. 8. Immunohistological analysis of temporal effects of single-dose A12 treatment on BxPC-3 xenograft tumors. Established tumors (300–400 mm^3) were removed at 1 and 6 h after a single 1-mg i.p. injection of A12 and processed for total IGF-IR, phosphorylated IGF-IR, and phosphorylated p44/42 MAPK. Control tumors were harvested at time 0, before injection. Tumor masses stained readily in control sections, surrounded by nonstaining mouse stroma, and showed marked reduction in staining intensity by 6 h after treatment. ×400.

in concert with IGF-IR overexpression, to generate autocrine activation of the IGF signaling pathway. Blocking signaling of both ligands is therefore likely to be necessary for an antagonist antibody to be an effective therapeutic.

We determined that after binding to IGF-IR on the surface of human tumor cells, A12 is internalized into cells and leads to the rapid degradation of the receptor by a lysosome-dependent pathway. In doing so, A12 caused a significant reduction in the relative levels of surface-associated IGF-IR on MCF7 cells, as demonstrated by fluorescence-activated cell-sorting analysis. This effect was not observed after incubation with IGF-I. The precise mechanism by which antibodies can act to target the IGF-IR for degradation in a manner distinct from ligand is unclear. However, the ability of A12 to block ligand signaling by two processes, direct antagonism of ligand binding and receptor surface down-modulation, may greatly enhance its effectiveness in suppressing IGF-IR signaling in tumor cells.

Anticancer therapeutic strategies using antibodies to target growth factor receptors have emerged as a new class of effective clinical therapeutics, providing efficacy with low toxicity as an alternative or supplement to conventional cytotoxic therapy (51, 52). The IGF-IR signaling pathway has been extensively demonstrated to be a causative factor in the development of many types of cancer. We have shown that A12 was capable of inhibiting IGF ligand signaling, mitogenesis, and proliferation in a variety of human tumor cell lines *in vitro*. Using three distinct tumor xenograft models, A12 was shown to effect a >70% inhibition of tumor growth *in vivo*. In the MCF7 breast cancer model, A12 effected a dose-dependent inhibition of tumor growth. These results support the concept that targeting IGF-IR may be beneficial in treating diverse tumor types. No toxicity or weight loss was observed in any of the A12-treated animals. However, because A12 was selected for binding to the human form of the IGF-IR, it is possible that the weak cross-reactivity it possesses for the mouse receptor may be insufficient to effect toxicity in mice. In addition, because A12 is an IgG1 antibody, it is possible that some of the antitumor activity may be due to immune effector functions. However, we have recently determined that A12 failed to stimulate natural killer cell-mediated lysis of target tumor cells in an antibody-dependent cellular cytotoxicity chromium release assay,[1] suggesting that the antitumor activity of A12 is due specifically to its function as an antagonist of the IGF-IR. In support of this, immunohistochemical analysis of tumor sections determined that a combination of both antiproliferative and proapoptotic processes was responsible for the reduction in tumor growth, and A12 could be demonstrated to effect a marked inhibition of total IGF-IR levels and phosphorylation after single-dose administration of the antibody.

Mechanistically, the fully human antibody A12 displays high affinity for the human IGF-IR and competes with its ligands, IGF-I and IGF-II, for binding. As a result, A12 inhibits ligand-mediated signal transduction of cell proliferation and survival pathways and dramatically inhibits tumor cell proliferation *in vitro* and *in vivo*. Because it is engineered as fully human monoclonal antibody, it is likely to exhibit low immunoreactivity in humans *in vivo* and therefore represents a good candidate molecule for therapeutic intervention in human diseases in which deregulated expression of the IGF-IR plays a critical role.

ACKNOWLEDGMENTS

We thank Venkat Mangalampalli and Anthony Kayas for antibody production support and Bridgett Finnerty for technical assistance with the immunohistochemistry studies.

REFERENCES

1. Adams, T. E., Epa, V. C., Garrett, T. P., and Ward, C. W. Structure and function of the type 1 insulin-like growth factor receptor. Cell. Mol. Life Sci., *57:* 1050–1093, 2000.
2. Baserga, R. The contradictions of the insulin-like growth factor 1 receptor. Oncogene, *19:* 5574–5581, 2000.

[1] D. L. Ludwig, unpublished results.

3. Nickerson, T., Chang, F., Lorimer, D., Smeekens, S. P., Sawyers, C. L., and Pollak, M. *In vivo* progression of LAPC-9 and LNCaP prostate cancer models to androgen independence is associated with increased expression of insulin-like growth factor I (IGF-I) and IGF-I receptor (IGF-IR). Cancer Res., *61:* 6276–6280, 2001.
4. Hellawell, G. O., Turner, G. D., Davies, D. R., Poulsom, R., Brewster, S. F., and Macaulay, V. M. Expression of the type 1 insulin-like growth factor receptor is up-regulated in primary prostate cancer and commonly persists in metastatic disease. Cancer Res., *62:* 2942–2950, 2002.
5. Gooch, J. L., Van Den Berg, C. L., and Yee, D. Insulin-like growth factor (IGF)-I rescues breast cancer cells from chemotherapy-induced cell death: proliferative and anti-apoptotic effects. Breast Cancer Res. Treat., *56:* 1–10, 1999.
6. Cullen, K. J., Yee, D., Sly, W. S., Perdue, J., Hampton, B., Lippman, M. E., and Rosen, N. Insulin-like growth factor receptor expression and function in human breast cancer. Cancer Res., *50:* 48–53, 1990.
7. Peyrat, J. P., and Bonneterre, J. Type 1 IGF receptor in human breast diseases. Breast Cancer Res. Treat., *22:* 59–67, 1992.
8. Lee, A. V., and Yee, D. Insulin-like growth factors and breast cancer. Biomed. Pharmacother., *49:* 415–421, 1995.
9. Hassan, A. B., and Macaulay, V. M. The insulin-like growth factor system as a therapeutic target in colorectal cancer. Ann. Oncol., *13:* 349–356, 2002.
10. Perer, E. S., Madan, A. K., Shurin, A., Zakris, E., Romeguera, K., Pang, Y., and Beech, D. J. Insulin-like growth factor I receptor antagonism augments response to chemoradiation therapy in colon cancer cells. J. Surg. Res., *94:* 1–5, 2000.
11. Wu, Y., Yakar, S., Zhao, L., Hennighausen, L., and LeRoith, D. Circulating insulin-like growth factor-I levels regulate colon cancer growth and metastasis. Cancer Res., *62:* 1030–1035, 2002.
12. Ge, N-L., and Rudikoff, S. Insulin-like growth factor I is a dual effector of multiple myeloma cell growth. Blood, *96:* 2856–2861, 2000.
13. All-Ericsson, C., Girnita, L., Seregard, S., Bartolazzi, A., Jager, M. J., and Larsson, O. Insulin-like growth factor-1 receptor in uveal melanoma: a predictor for metastatic disease and a potential therapeutic target. Investig. Ophthalmol. Vis. Sci., *43:* 1–8, 2002.
14. Yee, D., Morales, F. R., Hamilton, T. C., and Von Hoff, D. D. Expression of insulin-like growth factor I, its binding proteins, and its receptor in ovarian cancer. Cancer Res., *51:* 5107–5112, 1991.
15. Quinn, K. A., Treston, A. M., Unsworth, E. J., Miller, M. J., Vos, M., Grimley, C., Battey, J., Mulshine, J. L., and Cuttitta, F. Insulin-like growth factor expression in human cancer cell lines. J. Biol. Chem., *271:* 11477–11483, 1996.
16. Pollak, M. Insulin-like growth factor physiology and cancer risk. Eur. J. Cancer, *36:* 1224–1228, 2000.
17. Yaginuma, Y., Nishiwaki, K., Kitamura, S., Hayashi, H., Sengoku, K., and Ishikawa, M. Relaxation of insulin-like growth factor-II gene imprinting in human gynecologic tumors. Oncology (Basel), *54:* 502–507, 1997.
18. Guerra, F. K., Eijan, A. M., Puricelli, L., Alonso, D. F., Bal de Kier Joffe, E., Kornblihgtt, A. R., Charreau, E. H., and Elizalde, P. V. Varying patterns of expression of insulin-like growth factors I and II and their receptors in murine mammary adenocarcinomas of different metastasizing ability. Int. J. Cancer, *65:* 812–820, 1996.
19. Blakesley, V. A., Butler, A. A., Koval, A. P., Okubo, Y., and LeRoith, D. IGF-I receptor function. *In:* R. G. Rosenfeld and C. T. Roberts, Jr. (eds.), The IGF System: Molecular Biology. Physiology, and Clinical Applications, pp. 143–163. Totowa, NJ: Humana Press, 1999.
20. Heron-Milhavet, L., Karas, M., Goldsmith, C. M., Baum, B. J., and LeRoith, D. Insulin-like growth factor-I (IGF-I) receptor activation rescues UV-damaged cells through a p38 signaling pathway. Potential role of the IGF-I receptor in DNA repair. J. Biol. Chem., *276:* 18185–18192, 2001.
21. Kulik, G., Klippel, A., and Weber, M. J. Antiapoptotic signalling by the insulin-like growth factor I receptor, phosphatidylinositol 3-kinase, and Akt. Mol. Cell. Biol., *17:* 1595–1606, 1997.
22. Turner, B. C., Haffty, B. G., Narayanan, L., Yuan, J., Havre, P. A., Gumbs, A. A., Kaplan, L., Burgaud, J. L., Carter, D., Baserga, R., and Glazer, P. M. Insulin-like growth factor-I receptor overexpression mediates cellular radioresistance and local breast cancer recurrence after lumpectomy and radiation. Cancer Res., *57:* 3079–3083, 1997.
23. Lu, Y., Zi, X., Zhao, Y., Mascarenhas, D., and Pollak, M. Insulin-like growth factor-I receptor signaling and resistance to trastuzumab (Herceptin). J. Natl. Cancer Inst. (Bethesda), *93:* 1852–1857, 2001.
24. Benini, S., Manara, M. C., Baldini, N., Cerisano, V., Serra, M., Mercuri, M., Lollini, P. L., Nanni, P., Picci, P., and Scotlandi, K. Inhibition of insulin-like growth factor I receptor increases the antitumor activity of doxorubicin and vincristine against Ewing's sarcoma cells. Clin. Cancer Res., *7:* 1790–1797, 2001.
25. Muller, M., Dietel, M., Turzynski, A., and Wiechen, K. Antisense phosphorothioate oligodeoxynucleotide down-regulation of the insulin-like growth factor I receptor in ovarian cancer cells. Int. J. Cancer, *77:* 567–571, 1998.
26. Pietrzkowski, Z., Wernicke, D., Porcu, P., Jameson, B. A., and Baserga, R. Inhibition of cellular proliferation by peptide analogues of insulin-like growth factor 1. Cancer Res., *52:* 6447–6451, 1992.
27. D'Ambrosio, C., Ferber, A., Resnicoff, M., and Baserga, R. A soluble insulin-like growth factor I receptor that induces apoptosis of tumor cells *in vivo* and inhibits tumorigenesis. Cancer Res., *56:* 4013–4020, 1996.
28. Haylor, J., Hickling, H., El Eter, E., Moir, A., Oldroyd, S., Hardisty, C., and El Nahas, A. M. JB3, an IGF-I receptor antagonist, inhibits early renal growth in diabetic and uninephrectomized rats. J. Am. Soc. Nephrol., *11:* 2027–2035, 2000.
29. Scotlandi, K., Avnet, S., Benini, S., Manara, M. C., Serra, M., Cerisano, V., Perdichizzi, S., Lollini, P. L., De Giovanni, C., Landuzzi, L., and Picci, P. Expression of an IGF-I receptor dominant negative mutant induces apoptosis, inhibits tumorigenesis and enhances chemosensitivity in Ewing's sarcoma cells. Int. J. Cancer, *101:* 11–16, 2002.
30. Arteaga, C. L., and Osborne, C. K. Growth inhibition of human breast cancer cells *in vitro* with an antibody against the type I somatomedin receptor. Cancer Res., *49:* 6237–6241, 1989.
31. Arteaga, C. L., Kitten, L. J., Coronado, E. B., Jacobs, S., Kull, F. C., Jr., Allred, D. C., and Osborne, C. K. Blockade of the type I somatomedin receptor inhibits growth of human breast cancer cells in athymic mice. J. Clin. Investig., *84:* 1418–1423, 1989.
32. Scotlandi, K., Benini, S., Nanni, P., Lollini, P. L., Nicoletti, G., Landuzzi, L., Serra, M., Manara, M. C., Picci, P., and Baldini, N. Blockage of insulin-like growth factor-I receptor inhibits the growth of Ewing's sarcoma in athymic mice. Cancer Res., *58:* 4127–4131, 1998.
33. Furlanetto, R. W., Harwell, S. E., and Baggs, R. B. Effects of insulin-like growth factor receptor inhibition on human melanomas in culture and in athymic mice. Cancer Res., *53:* 2522–2526, 1993.
34. Kalebic, T., Tsokos, M., and Helman, L. J. *In vivo* treatment with antibody against IGF-1 receptor suppresses growth of human rhabdomyosarcoma and down-regulates p34cdc2. Cancer Res., *54:* 5531–5534, 1994.
35. Li, S. L., Liang, S. J., Guo, N., Wu, A. M., and Fujita-Yamaguchi, Y. Single-chain antibodies against human insulin-like growth factor I receptor: expression, purification, and effect on tumor growth. Cancer Immunol. Immunother., *49:* 243–252, 2000.
36. Park, J. W., and Smolen, J. S. Monoclonal antibody therapy. *In:* E. M. Scolnick (ed.), Advances in Protein Chemistry, Vol. 56. Drug Discovery and Design, pp. 360–421. San Diego, CA: Academic Press, 2001.
37. de Haard, H. J., van Neer, N., Reurs, A., Hufton, S. E., Roovers, R. C., Henderikx, P., de Bruine, A. P., Arends, J. W., and Hoogenboom, H. R. A large non-immunized human Fab fragment phage library that permits rapid isolation and kinetic analysis of high affinity antibodies. J. Biol. Chem., *274:* 18218–18230, 1999.
38. Lu, D., Jimenez, X., Zhang, H., Bohlen, P., Witte, L., and Zhu, Z. Selection of high affinity human neutralizing antibodies to VEGFR2 from a large antibody phage display library for antiangiogenesis therapy. Int. J. Cancer, *97:* 393–399, 2002.
39. Prager, D., Li, H. L., Asa, S., and Melmed, S. Dominant negative inhibition of tumorigenesis *in vivo* by human insulin-like growth factor I receptor mutant. Proc. Natl. Acad. Sci. USA, *91:* 2181–2185, 1994.
40. Casella, S. J ., Han, V. K., D'Ercole, A. J., Svoboda, M. E., and Van Wyk, J. J. Insulin-like growth factor II binding to the type I somatomedin receptor. Evidence for two high affinity binding sites. J. Biol. Chem., *261:* 9268–9273, 1986.
41. Siddle, K., Urso, B., Niesler, C. A., Cope, D. L., Molina, L., Surinya, K. H., and Soos, M. A. Specificity in ligand binding and intracellular signalling by insulin and insulin-like growth factor receptors. Biochem. Soc. Trans., *29:* 513–525, 2001.
42. Chames, P., Willemsen, R. A., Rojas, G., Dieckmann, D., Rem, L., Schuler, G., Bolhuis, R. L., and Hoogenboom, H. R. TCR-like human antibodies expressed on human CTLs mediate antibody affinity-dependent cytolytic activity. J. Immunol., *169:* 1110–1118, 2002.
43. Zhu, Z., Hattori, K., Zhang, H., Jimenez, X., Ludwig, D. L., Dias, S., Kussie, P., Koo, H., Kim, H. J., Lu, D., Liu, M., Tejada, R., Friedrich, M., Bohlen, P., Witte, L., and Rafii, S. Inhibition of human leukemia in an animal model with human antibodies directed against vascular endothelial growth factor receptor 2. Correlation between antibody affinity and biological activity. Leukemia (Baltimore), *17:* 604–611, 2003.
44. Pandini, G., Vigneri, R., Costantino, A., Frasca, F., Ippolito, A., Fujita-Yamaguchi, Y., Siddle, K., Goldfine, I. D., and Belfiore, A. Insulin and insulin-like growth factor-I (IGF-I) receptor overexpression in breast cancers leads to insulin/IGF-I hybrid receptor overexpression: evidence for a second mechanism of IGF-I signaling. Clin. Cancer Res., *5:* 1935–1944, 1999.
45. Hailey, J., Maxwell, E., Koukouras, K., Bishop, W. R., Pachter, J. A., and Wang, Y. Neutralizing anti-insulin-like growth factor receptor 1 antibodies inhibit receptor function and induce receptor degradation in tumor cells. Mol. Cancer Ther., *1:* 1349–1353, 2002.
46. Jansson, M., Hallen, D., Koho, H., Andersson, G., Berghard, L., Heidrich, J., Nyberg, E., Uhlen, M., Kordel, J., and Nilsson, B. Characterization of ligand binding of a soluble human insulin-like growth factor I receptor variant suggests a ligand-induced conformational change. J. Biol. Chem., *272:* 8189–8197, 1997.
47. Werner, H. Molecular biology of the type I IGF receptor. *In:* R. G. Rosenfeld and C. T. Roberts, Jr. (eds.), The IGF System: Molecular Biology, Physiology, and Clinical Applications, pp. 63–88. Totowa, NJ: Humana Press, 1999.
48. Milazzo, G., Yip, C. C., Maddux, B. A., Vigneri, R., and Goldfine, I. D. High-affinity insulin binding to an atypical insulin-like growth factor-I receptor in human breast cancer cells. J. Clin. Investig., *89:* 899–908, 1992.
49. Kato, H., Faria, T. N., Stannard, B., Roberts, C. T., Jr., and LeRoith, D. Role of tyrosine kinase activity in signal transduction by the insulin-like growth factor-I (IGF-I) receptor. Characterization of kinase-deficient IGF-I receptors and the action of an IGF-I-mimetic antibody (α IR-3). J. Biol. Chem., *268:* 2655–2661, 1993.
50. Sachdev, D., Li, S. L., Hartell, J. S., Fujita-Yamaguchi, Y., Miller, J. S., and Yee, D. A chimeric humanized single-chain antibody against the type I insulin-like growth factor (IGF) receptor renders breast cancer cells refractory to the mitogenic effects of IGF-I. Cancer Res., *63:* 627–635, 2003.
51. Nahta, R., Hortobagyi, G. N., and Esteva, F. J. Growth factor receptors in breast cancer: potential for therapeutic intervention. Oncologist, *8:* 5–17, 2003.
52. Cohen, R. B. Epidermal growth factor receptor as a therapeutic target in colorectal cancer. Clin. Colorectal Cancer, *2:* 246–251, 2003.
53. Vaughan, T. J., Osbourn, J. K., and Tempest, P. R. Human antibodies by design. Nat. Biotechnol., *16:* 535–539, 1998.